LATINO: A semi-classical model to study nuclear fragmentation

Article *in* Revista Mexicana de Fisica · October 1999

CITATIONS
20

READS
21

5 authors, including:

Ariel Chernomoretz
University of Buenos Aires
75 PUBLICATIONS **588** CITATIONS
SEE PROFILE

Claudio Dorso
University of Buenos Aires
152 PUBLICATIONS **1,821** CITATIONS
SEE PROFILE

Jorge Alberto Lopez
University of Texas at El Paso
153 PUBLICATIONS **1,028** CITATIONS
SEE PROFILE

LATINO: A semi-classical model to study nuclear fragmentation

A. Barrañón
Departamento de Ciencias Básicas, Universidad Autonoma Metropolitana-Azcapotzalco, México, D.F., Mexico

A. Chernomoretz and C.O. Dorso
Departamento de Física, Facultad de Ciencias Exactas y Naturales, Universidad de Buenos Aires Nuñez 1428, Buenos Aires, Argentina

J.A. López and J. Morales
Department of Physics, University of Texas at El Paso, El Paso, Texas 79968, U.S.A.

Recibido el 7 de enero de 1999; aceptado el 10 de marzo de 1999

Several characteristics of heavy-ion reactions at intermediate energies, such as the formation of an intermediate residue, or neck-like structure, are not well understood. To study this and other features of heavy-ion collisions and their fragmentation, a semi-classical model based on the use of molecular dynamics is presented. The model uses a two-body potential developed to reproduce nucleon-nucleon cross sections realistically. Preliminary results of the use of the model to study the caloric curve of nuclear matter, formation of necks, as well as the temperature evolution of the system are discussed.

Keywords: Nuclear fragmentation; molecular dynamics; nuclear reactions

Varias características de reacciones de iones pesados a energías intermedias, tales como la formación de residuos intermediarios, o estructuras de cuello, no son bien entendidas. Para estudiar estas y otras características de colisiones de iones pesados y su fragmentación, un modelo semi-clásico basado en el uso de dinámica molecular es presentado. El modelo usa un potential de dos cuerpos desarrollado para reproducir secciones transversales de nucleón-nucleón de una manera realista. Resultados preliminares del uso de este modelo para estudiar la curva calórica de la materia nuclear, la formación de cuellos, asi como la evolución de la temperatura del sistema son discutidos.

Descriptores: Fragmentación nuclear; dinámica molecular; reacciones nucleares

PACS: 25.70.Pq

1. Introduction

The investigation of fragmentation ocurring in heavy ion collisions at energies between 10 and 100 MeV/nucleon has been the subject of many studies [1–15]. Until recently, only a fraction of the large number of fragments produced in collisions were detected. Newer detector arrays with larger angular coverage [16–20] make now possible a more complete detection of the charged particles produced in the reaction.

With these richer data it is now evident that the reaction dynamics plays an important role in the breakup [21–29]. These measurements show, for instance, that the binary character of the reaction exists at the Fermi energy (10 MeV/nucleon $< E_{beam} <$100 MeV/nucleon) [30–35]. Another not-well-understood observable at these energies is the formation of an intermediate residue, or neck-like structure, usually involving very heavy ions [36–40]. This structure could be the low-energy beginning of the mid-rapidity source usually observed in higher-energy heavy ion reactions [41–44].

Although many theoretical models, even with conflicting assumptions, used to explain inclusive data, these newer data show features out of reach for most calculational theories. The models used to study the fragmentation process can be casted in two categories: slow and promtp breakup. Several models [45–48] assume that the fragments are emitted one at a time from an excited system in a sequence of fission-like decays. This decay method is known to be the main de-excitation mechanism in low-energy fission reactions. However, these models are based on nucleon exchange and on sequential evaporation, and thus do not allow, for instance, for the formation of intermediate residues.

Other models (such as the evaporation-condensation model [49], the liquid-gas phase transition model [50], the spinodal decomposition model [51], and others statistical ones [50, 5, 6]) used a rapid approach to fragment formation. Forming a compressed system that expands and disassembles, leads to a prompt formation of nuclear clusters. These scenarios allow for a possible formation of hot participant regions, such as the observed necks. We now focus our attention on these microscopic dynamic models.

1.1. Dynamical models: BUU and QMD

Amongst the most popular models to describe heavy-ion collisions at intermediate energy are the Boltzmann-Uehling-Uhlenbeck (BUU) and Quantum Molecular Dynamics (QMD) models.

The BUU model [52] calculates the one-body phase-space density function, but does not incorporate higher-order

The polarization phenomena associated with a molecular state implies that it should be associated with dipole excitations of the separation vector. In this case expectation values of the dipole operator do not vanish as the center of mass and center of charge of the polarized molecular state do not coincide. Hence molecular states give rise to low lying dipole excitations. While the high lying Giant Dipole Resonace (GDR) is associated with (a Goldhaber-Teller) excitation of the neutron distribution against that of the proton, a molecular excitation involves a smaller fraction of the nucleons at the surface and is thus expected to occur at lower excitation; i.e. a soft dipole mode.

The GDR excitation exhausts the (TRK) energy weighted dipole sum rule:

$$S_1(E1;A) = \Sigma_i\, B(E1: 0^+ \rightarrow 1_i^-) \times E^*(1_i^-) = \frac{9}{4\pi}\,\frac{NZ}{A}\,\frac{e^2\hbar^2}{2m}. \quad (3)$$

And for a molecular state Alhassid, Gai, and Bertsch [19] derived sum rules by subtracting the individual sum rules of the contituents from the total sum rule:

$$S_1(E1;A_1+A_2) = S_1(A) - S_1(A_1) - S_1(A_2), = \frac{Z_1A_2 - A_1Z_2}{AA_1A_2}\,\frac{e^2\hbar^2}{2m}, \quad (4)$$

$$S_1(E1;\alpha+A_2) = \frac{(N-Z)^2}{A(A-4)}\,\frac{e^2\hbar^2}{2m},$$

$$S_1(E1;n+A_2) = \frac{Z^2}{A(A-1)}\,\frac{e^2\hbar^2}{2m},$$

$$S_1(E1;2n+A_2) = \frac{2Z^2}{A(A-2)}\,\frac{e^2\hbar^2}{2m}. \quad (5)$$

Note that the sum rule for two neutrons molecular states, $S_1(2n+A_2)$, is the same whether one assumes a "di-atomic" nuclear molecule (^{9}Li+ a dineutron), or a "tri-atomic" nuclear molecule (^{9}Li+n + n). And the sum rule (as a kinematical model) does not allow us to distinguish between the two molecular cases. These molecular sum rules (Eqs. 4 and 5) were shown to be useful in elucidating molecular (cluster) states in ^{18}O where the measured $B(E1)$'s and $B(E2)$'s exhaust 13% and 23%, respectively, of the molecular sum rule [20]. Similarily, these molecular states in ^{18}O have alpha widths that exhaust 20% of the Wigner sum rule. The branching ratios for electromagnetic decays in ^{18}O were also shown to be consistent with predictions of the Vibron model in the U(3) limit [21]. Indeed the manifestation of a molecular structure in ^{18}O has altered our undertsanding of the coexistence of degrees of freedoms in ^{18}O [22].

The dipole strength at approximately 1.2 MeV in ^{11}Li, shown in Fig. 1, exhausts 20% of the two neutrons molecular sum rule, and the total strength integrated up to 5 MeV exhausts 100% of that sum rule. We emphasize that the experimental efficiency at for example 6.0 MeV is very large (30%) [1], but no strength is found at higher energies beyond 100% of the molecular sum rule. These two facts strongly suggest the existence of a low lying soft dipole mode in ^{11}Li.

6. Conclusion

In conclusions we demonstrate that quantitative tools exist to test the validity of the "threshold effect" and the "soft dipole mode" interpretation of the dipole ($E1$) strength in ^{11}Li. More precise data are needed to rule out one or the other interpretation and this paper may serve as an impetus for such data. Current interpration is consistent with the existence of a low lying dipole mode in ^{11}Li at approximately 1.2 MeV, and may pose difficulties to other interpretations.

Acknowledgments

Work supported by USDOE Grant No. DE-FG02-94ER40870.

* Invited talk, XXII Symposium on Nuclear Physics, Jan. 6-9, 1999, Oaxtepec, México.

1. M. Zinser *et al.*, *Nucl. Phys.* **A619** (1997) 151.
2. K. Ikeda *Nucl. Phys.* **A538** (1992) 355c.
3. P.G. Hansen, *Nucl. Phys.* **A588** (1995) 1c; P.G. Hansen and A.S. Jensen, *Annu. Rev. Nucl. Part. Sci.* **45** (1995) 591.
4. A.A. Korsheninnikov *et al.*, *Phys. Rev. Lett.* **78** (1997) 2317.
5. T. Kobayashi, *Phys. Lett. A* **538** (1992) 343c.
6. M.G. Gornov *et al.*, *Phys. Rev. Lett.* **81** (1998) 4325.
7. S. Karataglidis *et al.*, *Phys. Rev. Lett.* **79** (1997) 1447.
8. J.M. Blatt and V.F. Weisskopf, *Theoretical Nuclear Physics*, (Wiley, New York, 1952).
9. F.L. Shapiro, JETP **7** (1958) 1132.
10. A.A. Bergman and F.L. Shapiro, *Sov. Jour. Phys.* JETP **13** (1961) 895.
11. S.B. Borazkov *et al.*, *Sov. Jour. Nucl. Phys.* **35** (1982) 307.
12. H.A. Bethe and C. Longmire, *Phys. Rev.* **77** (1950) 647.
13. M. Heil, F. Kappler, M. Wiescher, A. Mengoni, *A. Phys. Jour.* **507** (1998) 997, and references therein.
14. F. Iachello and R.D. Levine, *Algebraic Theory of Molecules*, (Oxford University Press, New York, 1995).
15. R.H. Dalitz, *Low and Intermediate Energy Kaon-Nucleus Physics*, (Oxford University Press, Oxford, 1981) p. 381.
16. J. Weinstein and N. Isgur, *Phys. Rev. Lett.* **48** (1982) 659.
17. F. Close, N. Isgur, and S. Kumano, *Nucl. Phys.* **B389** (1993) 513.
18. F. Iachello and A.D. Jackson, *Phys. Lett.* **108B** (1982) 151.
19. Y. Alhassid, M. Gai, and G.F. Bertsch, *Phys. Rev. Lett.* **49** (1982) 1482.
20. M. Gai *et.al.*, *Phys. Rev. Lett.* **50** (1983) 239.
21. M. Gai *et al.*, *Phys. Rev.* C **43** (1991) 2127.
22. M. Gai *et al.*, *Phys. Rev. Lett.* **62** (1989) 874.

correlations and shows difficulties in producing fragmentation. BUU calculations have failed in yielding neck fragments or an intermediate residue in semi-peripheral collisions [40]. The closest approach has been the study case of Colonna *et al.* [53] who introduced an *ad-hoc* random fluctuating term into BUU, and predicted the existence of an intermediate neck which led to the emission of fragments from the region.

The QMD model [54] includes nucleon correlations (by following the time evolution of the collision) while incorporating, also in an *ad-hoc* manner, some quantum features. QMD describes fluctuations leading to a fragmentation of the nuclear system, but fails to reproduce the fragment multiplicities experimentally observed.

Although the QMD model [55] yields well defined ground states and more stable initial nuclei, to describe the long-time behavior of fragments produced, the model needs to be coupled to a second statistical model in a somewhat arbitrary manner. Recent efforts to identify neck-like fragment sources [40] using this two-model structure found many two-fragment events and few three-source events. The three-fragment cases observed corresponded to collisions with a dissipative binary process producing target-like and projectile-like fragments plus evaporation particles.

The BUU and QMD-Statistical Decay models both fail in producing enough fragments with the proper middle rapidity to describe the formation of necks. A successful model should include all-order nucleon-nucleon correlations (to form fragments), should be able to include all of the collision-induced correlations (to form necks), as well as the nucleon dynamics at the proper kinetic energies (to reproduce the collision realistically). A search for such a model motivates the present study.

2. The model

Out of the various methods used to study heavy ion reactions (*e.g.* BUU, VUU, Landau-Vlasov, *etc.*, see Ref. 50), only molecular dynamics (MD) can describe changes of phase, hydrodynamic flow, and non-equilibrium dynamics, without adjustable parameters. In the present work, we use a simple MD model with a two-body potential developed to reproduce nucleon-nucleon cross sections realistically. Although the main ingredients of the model were developed in Illinois [56], we have nicknamed the working model, *i.e.* the MD codes plus the fragment-recognition algorithm, LATINO due to the multi-Latin American composition of the present collaboration.

The model used in this work was developed to study the accuracy of the Vlasov-Nordheim approximation. The model was found to give the empirical energy and density of nuclear matter. Of special interest to this work is the fact that the n-n, n-p, and p-p potentials have been adjusted to produce realistic effective scattering cross sections. For our analysis of finite nuclei, the Coulomb term is also included. For a complete description of the potential see reference [56].

The "nuclear" part of the interaction potential is :

$$V_{np}(r) = V_r \left[\frac{\exp(-\mu_r r)}{r} - \frac{\exp(-\mu_r r_c)}{r_c}\right] - V_a \left[\frac{\exp(-\mu_a r)}{r} - \frac{\exp(-\mu_a r_a)}{r_a}\right]$$

$$V_{nn}(r) = V_{pp}(r) = V_0 \left[\frac{\exp(-\mu_0 r)}{r} - \frac{\exp(-\mu_0 r_c)}{r_c}\right] \quad (1)$$

where $r_c = 5.4$ fm is a cutoff radius, V_{np} is the potential acting between a neutron and a proton while V_{nn} is the potential acting between two identical nucleons.

The first interaction is attractive at large r and repulsive at small r, while the latter is purely repulsive. In this way, no bound state of identical nucleons can exist. The values of the parameters of the Yukawa potentials are given in Ref. 56 and give a corresponding equation of state (EOS) of classical matter with a compressibility of about 250 MeV (set M in Ref. 56). This EOS strongly resembles the one expected for nuclear matter (i.e. equilibrium density $\rho_0 = 0.16$ fm^{-3} and energy $E(\rho_0) = -16$ MeV/nucleon). Furthermore, it was shown that many experimental data on heavy-ion collisions are reasonably explained by this classical model. Of course this is not accidental, but due to the accurate choice of the parameters of the two-body potentials.

2.1. Numerical experiments

Two kinds of numerical experiments are performed in the present study. First we study the time evolution of isolated nuclei that are isotropically excited, second we analyze the time evolution of excited systems resulting from the collision of a light projectile on a heavy target.

The nuclei to be used in our computational experiments, are nuclei-like systems built with the right number of protons and neutrons. These nuclei are produced on the ground state using molecular dynamics. To allow the system reach its most favorable configuration, a nuclear system is produced at a rather high temperature confined in a steep spherical potential. The system then is allowed to cool down until it reaches a self-contained state. At this point the confining potential is removed and the system is further cooled down until a reasonable binding energy is attained

With this model we study both isolated excited systems and collisions. For isolated systems we study the time evolution of highly excited states in the following way. Starting with a system in its ground state, an excited system is produced by randomly assigning momenta to the constituent particles according to a Maxwell Boltzmann distribution at the desired temperature. Due to the small size of the system, a small adjustment, via scaling of the momenta, is needed to insure that all initial conditions happen to be at exactly the same temperature.

To study collisions, we use molecular dynamics calculations in which the center-of-mass velocity of the projectile is

boosted to the desired energy. Everytime a collision is performed, the relative orientations of the projectile and target are randomly selected by rotations with random values of the corresponding Euler angles.

In both cases the evolution of the total system is followed integrating the Newton's equations of motion using a standard velocity-Verlet algorithm. The integration step is carefully chosen in order to achieve an energy conservation of the order of 0.01%.

2.2. Detecting fragments

For an eventual comparison to experiments, the nucleon information needs to be transformed into fragment information. While detecting fragments at asymptotic times is trivial, the identification of fragments as a function of time is a rather complicated problem. Moreover it becomes crucial to be able to determine the times at which fragments are formed, and/or emitted. Such a knowledge allows us to explore, for example, the caloric curve in fragmentation. A step in this direction was given in Ref. 57 where the so called Early Cluster Formation Model was formulated. With this model it was found that the final asymptotic fragments are conceived very early in the evolution, when the system is still dense in configurational space. Density fluctuations in phase space were found to be the precursors of asymptotic fragments.

Clusters at this early stage of the evolution are associated with the most bound density fluctuations in phase space according to the following definition. The prefragments are that partition of the system for which :

$$e = \sum_{C} \left[\sum_{i \epsilon C} \frac{(p_i^{\rm cm})^2}{2m} + \sum_{i \epsilon C, j \epsilon C, i>j} V_{ij} \right] \qquad (2)$$

attains its minimum. Here, C denotes the elements of a given partition, e the total binding energy of the elements of the partition, and $p_i^{\rm cm}$ is the momentum of particle i calculated in the center of momentum of the element C of the partition .

Since the momenta are to be calculated in the center of momentum of the fragments, this is not a trivial problem. Nevertheless, the problem can be tackled with the use of simulated annealing techniques. Here we use a fragment recognition algorithm, Early Cluster Recognition Algorithm or ECRA, adapted for the interaction potential of our case.

As a reference, we also calculate the so-called configurational clusters. They are defined in the following way: given a cluster C, the following relation is satisfied:

$$\underset{i \epsilon C}{\forall} \; \underset{j \epsilon C}{\exists} \; (r_i - r_j) < r_c \qquad (3)$$

where i, j denote particle index, and r_c is the clusterization radius. We will refer to this algorithm as the minimum spanning tree, or MST.

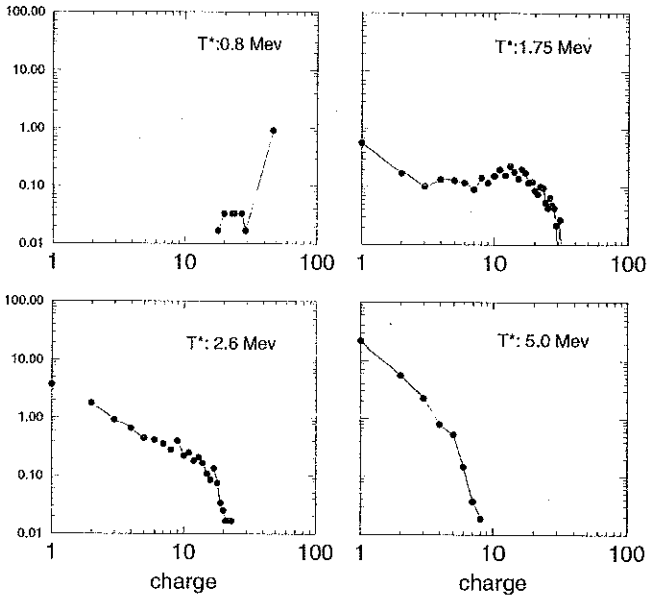

FIGURE 1. Charge spectra for exploding Ag like systems at four different initial temperatures, from left to right and top to bottom, 0.8, 1.75, 2.6 and 5 MeV.

3. Preliminary results

A study of the excitation energy predicted by LATINO in the reaction ^{3} He on ^{107}Ag at 1.8 GeV/nucleon was presented in Ref. 58. In this section we briefly list a few other preliminary results.

3.1. Time scales of fragment formation

The fragmentation time scales can be characterized by the time evolution of fragment sizes. As this varies for different energies, the charge spectra obtained for disassembling excited nuclei at several energies is presented first.

In Fig. 1 we show the charge spectra produced by exploding Ag nuclei with different initial temperatures, namely T = 0.8 MeV, 1.75 MeV, 2.6 MeV and 5 MeV. It can be clearly seen that an evolution from fission like to exponentially decaying spectra is found. Also notice that at $T = 2.6$ MeV the spectra gets close to power law like.

Figure 2 shows the time evolution of relevant observables. First, the time evolution of the size of the maximum fragment is presented. Both fragment definitions (ECRA and MST) are used for three different initial temperatures of the excited system, namely 2.6, 3 and 5 MeV. It can be seen that, as found in other calculations like QMD and for Lennard-Jones systems, the maximum fragment is formed very early in the evolution of the system. Moreover it can be readily observed that the typical time scales for this potential are very long.

In Fig. 3 a more detailed analysis of the fragmentation process is presented showing, as a function of time, the average population of different mass bins. Once again the fragments are seen to form very fast in phase space, but it takes

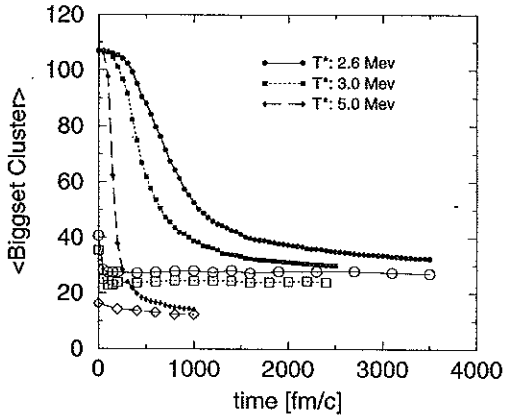

FIGURE 2. Time evolution of the maximum fragment according to MST (full symbols) and ECRA (empty), for three different initial temperatures (circles 2.6 MeV; squares 3 MeV and diamonds 5 MeV) . It can readily be seen that the mean value of the maximum fragment size reaches its asymptotic value very early in the evolution.

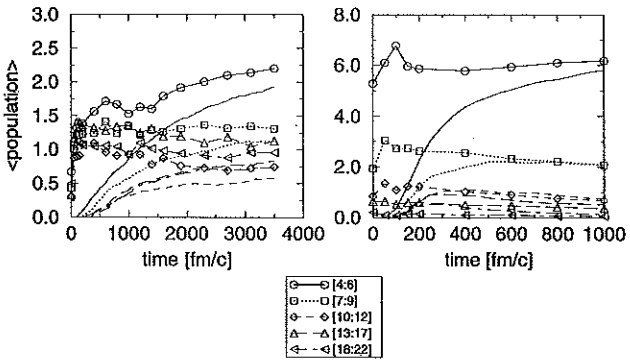

FIGURE 3. Time dependence of the population of different mass bins according to ECRA (empty symbols) and MST. Masses from 4 to 6 are represented by full lines, 7–9 by dots, 10–12 by a dashed line, 13–17 by a long-dashed line, and 18–22 by a dot-dashed line.

a long time for them to become separated in configurational space. This effect is probably due to the slow development, in configurational space, of Coulomb instabilities.

3.2. Fragment temperatures

In the recent debate about the calculation of the caloric curve in nuclear fragmentation, different thermometers give rise to very different interpretation of experimental data. For example, while the determination of the fragmentation temperature out of double ratios [59] indicate a "rise-plateau" pattern (which resembles the standard, thermodinamic caloric curve for infinite systems), temperatures calculated from excited-state population-ratios of small clusters indicate a "rise-plateau" kind of caloric curve [60].

In a previous work [61] (for the case of fragmentation of hot Lennard-Jones drops) it was observed that the time of fragment formation could be precisely determined. In order to achieve this goal different time scales were defined:

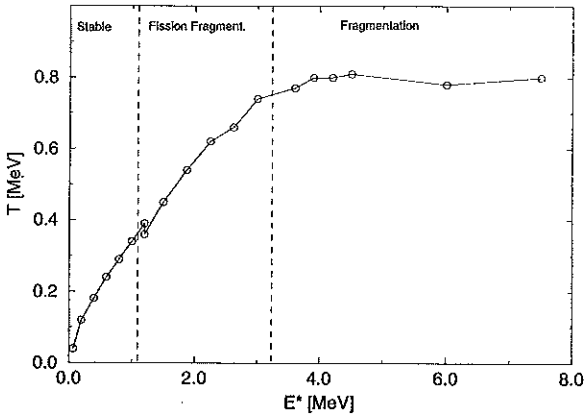

FIGURE 4. Asymptotic mean cluster temperature as a function of excitation energy. The temperatures were obtained as an average over masses bigger than 6 (full circles). For energies above 3.0 MeV the cluster temperatures are independent of the excitation energy of the system. Also shown is a preliminary estimation of the local temperature obtained from the time of stabilization of the fragment spectra (see text).

i) the time of fragment formation τ_{ff}, associated to that stage of the evolution at which the ECRA fragments attained microscopic stability, and

ii) the time of fragment emission τ_{fe} related to the time at which configurational fragments reached microscopic stability.

It is always true that $\tau_{ff} < \tau_{fe}$ which means that fragments are formed in the early dense stage of the evolution. It was also seen that the system attained local equilibrium at times of the order of τ_{ff}. Temperatures calculated at this times displayed a "rise-plateau" pattern, which means that for excitation energies above a given threshold the temperature of the system at fragmentation time was independent of the energy deposited on it. Moreover this temperature was strongly related to the corresponding temperature of the formed fragments [61].

Taking these results as a reference we perform the same kind of calculation for the present potential. For this purpose we will study the time evolution of excited drops of particles interacting via the Pandharipande potential plus Coulomb, with an isotopic composition similar to Ag. The time evolution of the system is followed for a very long time. The fragment structure of the configurations is obtained by applying the already described ECRA analysis. Once the fragments have been recognized its temperature is calculated according to:

$$T_{\rm int}(n,t) = 3D\frac{1}{N_n}\sum_i \frac{2}{n_l}\sum_{j\in i}\frac{1}{2}m\left[\mathbf{v}_j^{(\rm cm)}\right]^2, \qquad (4)$$

with n_l, the number of degrees of freedom, for three-dimensional fragments the mass number is $n > 2$, the linear and angular momentum have been removed and are conserved so $n_l = 3n - 6$.

In Fig. 4 we show the mean temperature of asymptotic clusters of mass bigger than 6 as a function of the excitation

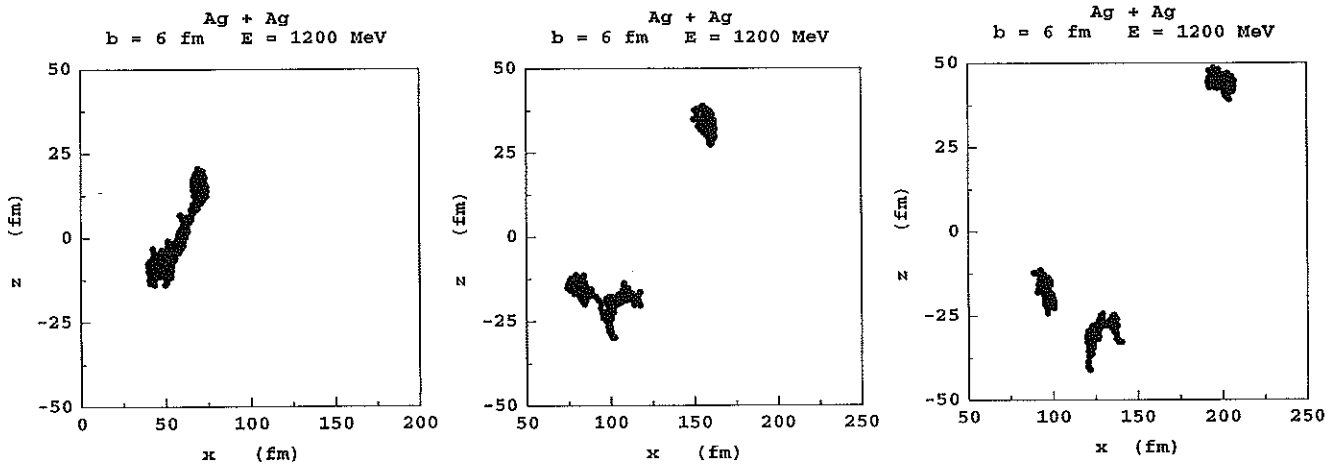

FIGURE 5. Evolution of the collision of Ag on Ag at $E = 1200$ MeV at an impact parameter of $b = 6$ fm. The plot shows the projection over the x-z plane. The formation of an intermediate residue, moving slower than the projectile, but faster than the target, is evident.

energy of the system. Three distinctive regions are marked in the figure: the first one corresponds to very low energy systems which remain stable for very long times ($E^* < 1$ MeV). For higher energies the system begins to be unstable against fission like processes and afterwards evaporation begins to compete as a de-excitation mechanism. Finally for energies above 3.2 MeV fragmentation becomes the dominating mode. It can also be seen that the temperature of the fragments rises monotonously up to approximately $E^* = 3.4$ MeV, and afterwards reaches a plateau.

3.3. Necks

Experimental signatures of the formation of an intermediate residue, with a velocity between that of the projectile-like emitter and that of the target-like emitter, has been investigated with reverse kinematic in nearly symmetric and asymmetric reactions under the same experimental set-up [40].

Studying the reactions ^{35}Cl + ^{12}C, ^{24}Mg and ^{197}Au at 43 MeV/nucleon, it was found that the formation of an intermediate residue appears in up to 40% of the detected events. In the same study [40] it was also determined that most common models (BUU and QMD) fail to produce enough neck structures. As the present model include all-order particle correlations and the collision-induced density and momentum fluctuations, the formation of intermediate residues should be expected.

Figure 5 shows three snapshots of the evolution of Ag colliding on Ag at $E = 1200$ MeV at an impact parameter of $b = 6$ fm. Clearly seen is the formation of an intermediate residue, or neck, that moves with a velocity smaller than that of the projectile, but larger than that of the target. The formation of three sources is evident.

3.4. Other features

More common features, such as the inclusive fragment multiplicity can also be obtained with LATINO. Figure 6 shows

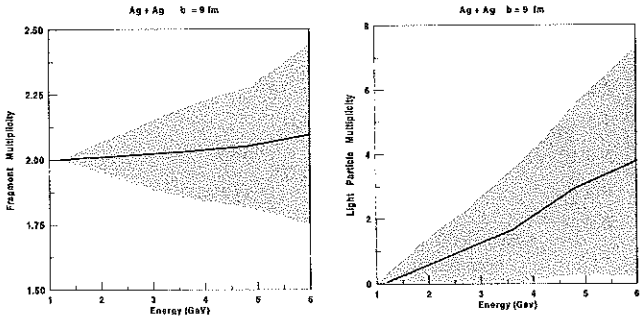

(a) (b)

FIGURE 6. Fragment (M_I) and light particle (M_L) multiplicities obtained with Latino as a function of beam energy for Ag on Ag at fixed impact parameter $b = 9$ fm. The shaded regions denote one standard deviation above and below the mean multiplicities (solid line).

the increase of the intermediate mass fragments [$A \geq 10$, panel a)] and the light particles [$A < 10$, panel b)], respectively, as a function of beam energy, for the reaction Ag on Ag at fixed impact parameter $b = 9$ fm. The shaded regions denote one standard deviation above and below the mean multiplicities (solid line). A comparison with real data would necessarily have to include the mix of data produced with different bs, as well as the use of the experimental filters.

4. Conclusions and perspectives

The model presented seems to be an effective tool in studying different aspects of heavy ion reactions.

With respect to the caloric curve, the results shown point in the direction of confirming that the shape of the caloric curve for fragmenting systems should be of the type "rise-plateau" with no "vapor branch", as already found for

Lennard-Jones systems. Nevertheless a more detailed analysis of times of fragment formation should be performed before final conclusions can by reached.

Necks are clearly formed under suitable conditions of energy and impact parameter. A more thorough study of these intermediate sources should help us understand their role in the fragment formation process.

Acknowledgments

Work supported by the National Science Foundation (PHY-96-00038) and the Universidad de Buenos Aires (EX-070). J.A.L. and J.M acknowledge the hospitality of the Universidad de Buenos Aires and C.O.D. that of the University of Texas at El Paso. We thank Christian Escudero and Azael Avalos for contributions to this work.

1. J.P. Bondorf *et al.*, *Nucl. Phys.* **A443** (1985) 321.
2. E. Suraud *et al.*, *Prog. of Part. & Nucl. Phys.* 1989.
3. D. Guerreau, GANIL P 89-07, Les Houches 89.
4. B. Tamain, *Enrico Fermi School, Course CXII, Italy 1989*, (Elsevier Science Publishers B.V., North-Holland, 1991).
5. J.A. López and J. Randrup, *Nucl Phys.* **503** (1989) 183; *Nucl Phys.* **512** (1990) 345; *Nucl Phys.* **571** (1994) 379.
6. D.H.E. Gross, *Rep. Prog. Phys.* **53** (1990) 605.
7. L.G. Moretto and G.J. Wozniak, *Ann. Rev. Nucl. Phys.* (1993).
8. W. Rosch *et al.*, *Nucl. Phys.* **A496** (1989) 141.
9. Y. Blumenfeld *et al.*, *Phys. Rev. Lett.* **66** (1991) 576.
10. C.A. Pruneau *et al.*, *Nucl. Phys.* **A534** (1991) 204.
11. B. Heide and H.W. Barz, *Phys. Lett. B* **337** (1994) 53.
12. L. Phair *et al.*, *Nucl. Phys.* **A548** (1992) 489.
13. D. Cussol *et al.*, *Nucl. Phys.* **A561** (1993) 298.
14. O. López *et al.*, *Phys. Lett. B* **315** (1993) 34.
15. K. Hagel *et al.*, *Phys. Rev. C* **50** (1994) 2017.
16. D.W. Stracener *et al.*, *Nucl. Instr. and Meth. in Phys. Res. A* **294** (1990) 485.
17. R.T. De Souza *et al.*, *Nucl. Instr. and Meth. in Phys. Res. A* **295** (1990) 109.
18. D. Drain *et al.*, *Nucl. Instrun. and Meth. in Phys. Res.* **A281** (1989) 528.
19. J. Pouthas *et al.*, *Nucl. Instrum. Meth.* **A357** (1994) 418.
20. D. Heuer *et al.*, *Phys. Rev.* C **50** (1994) 1943.
21. D. Jouan *et al.*, *Z. Phys. A* **340** (1991) 63.
22. M. Colonna, N. Colonna, A. Bonasera, and M. DiToro, *Nucl. Phys.* **A541** (1992) 295.
23. J. Suro *et al.*, Schmidt, *Nucl. Phys.* **A548** (1992) 353.
24. R. Wada *et al.*, *Nucl. Phys.* **A548** (1992) 471.
25. C. Schwartz *et al.*, *Z. Phys. A* **345** (1993) 29.
26. G. Peilert, H. Stöcker, and W. Greiner, *Rep. Prog. Phys.* **57** (1994) 533.
27. H. Fuchs and K. Möhring, *Rep. Prog. Phys.* **57** (1994) 231.
28. S.P. Baldwin *et al.*, *Phys. Rev. Lett.* **74** (1995) 1299.
29. Y. Larochelle *et al.*, *Phys. Rev. C* **53** (1996) 823.
30. B. Lott *et al.*, *Phys. Rev. Lett.* **68** (1992) 3141.
31. B.M. Quednau *et al.*, *Phys. Lett. B* **309** (1993) 10.
32. J.F. Lecolley *et al.*, *Phys. Lett. B* **325** (1994) 317.
33. Y. Larochelle *et al.*, *Phys. Lett. B* **352** (1995) 8.
34. J. Péter *et al.*, *Nucl. Phys.* **A593** (1995) 95.
35. L. Beaulieu *et al.*, preprint TASCC-P-96-2 (1996).
36. C.A. Pruneau *et al.*, *Nucl. Phys.* **A534** (1991) 204.
37. C.P. Montoya *et al.*, *Phys. Rev. Lett.* **73** (1994) 3070.
38. J. T oke *et al.*, *Phys. Rev. Lett.* **75** (1995) 2920.
39. J.F. Lecolley *et al.*, *Phys. Lett. B* **354** (1995) 202.
40. Y. Larochelle *et al.*, *Phys. Rev. C* **55** (1997) 1869.
41. G.D. Westfall *et al.*, *Phys. Rev. Lett.* **37** (1976) 1202.
42. R. Stock, *Phys. Rep.* **135** (1986) 259.
43. B. Borderie, M.F. Rivet, and L. Tassan-Got, *Ann. Phys. Fr.* **15** (1990) 287.
44. J.P. Alard *et al.*, *Phys. Rev. Lett.* **69** (1992) 889.
45. R.J. Charity *et al.*, *Nucl. Phys.* **A483** (1988) 371.
46. J.A. López and J. Randrup, *Nucl. Phys.* **A491** (1989) 477; J.A. López and J. Randrup, *Comp. Phys. Comm.* **70** (1990) 92.
47. C.H. Dasso and G. Pollarolo, *Comp. Phys. Comm.* **50** (1988) 341.
48. R.J. Charity *et al.*, *Nucl. Phys.* **A483** (1988) 371.
49. A.L. Goodman, J.I. Kapusta, and A.Z. Mejkian, *Phys. Rev. C* **30** (1984) 851.
50. W. Bauer and J. Kapusta, eds., *Advances in Nuclear Dynamics*, (World Scientific, Singapore, 1991) and references therein.
51. G. Bertsch, and P.J. Siemens, *Phys. Lett. B* **126** (1983) 9; J.A. López and P.J. Siemens, *Nucl. Phys.* **A431** (1984) 728.
52. G.F. Bertsch and S. Das Gupta, *Phys. Rep.* **160** (1988) 190.
53. M. Colonna, M. Di Toro, and A. Guarnera, *Nucl. Phys.* **A589** (1995) 160.
54. J. Aichelin and H. Stöcker, *Phys. Lett. B* **176** (1986) 14.
55. G. Peilert *et al.*, *Phys. Rev. C* **46** (1992) 1404.
56. R.J. Lenk, T.J. Schlagel, and V.R. Pandharipande, *Phys. Rev. C* **42** (1990) 372.
57. C.O. Dorso and J. Randrup *Phys. Rev.* C **301** (1993) 328.
58. C.O. Dorso, J.A. López, and J. Morales, Bull. *Am. Phys. Soc.*, **43** (1998) 1211.
59. S. Albergo, S. Costa, E. Costanzo and A. Rubbino, *Il Nouvo Cimento* **A89** (1985)1.
60. V. Serfling *et al. Phys. Rev. Lett.* **80** (1998) 3928.
61. A. Strachan and C.O. Dorso, *Phys. Rev. C* **58** (1998) R632; A. Strachan and C.O. Dorso, *Phys. Rev. C* **59** (1999) 285.